Eur. Phys. J. D **42**, 163–177 (2007)
DOI: 10.1140/epjd/e2006-00274-0

THE EUROPEAN PHYSICAL JOURNAL D

# Spontaneous emission from a ladder three-level atom in anisotropic photonic crystals

S.Y. Xie[1,a] and Y.P. Yang[1,2]

[1] Department of Physics, Tongji University, Shanghai 200092, P.R. China
[2] Institute for Quantum Studies and Department of Physics, Texas A&M University, College Station, TX 77843, USA

Received 19 June 2006
Published online 22 December 2006 – 

**Abstract.** We investigate the spontaneous radiation from a ladder three-level atom embedded in a three-dimensional anisotropic photonic crystal with an external driving field. The properties of the spontaneous emission are dependent strongly on the relative position of the middle level from the band edge. Due to the Autler-Townes splitting by the action of the driving field, the external driving field can also affect the properties of the spontaneous emission. The population exchanged between the upper and the middle levels decreases as the detuning of the external driving field frequency from the corresponding transition frequency increases. The properties of the emission field can be changed or so much as controlled by choosing suitable intensity of the external driving field. The emission spectrum is more complex, and dependent on the location of the observer in this case.

**PACS.** 42.50.Dv Nonclassical states of the electromagnetic field, including entangled photon states; quantum state engineering and measurements – 32.80.Bx Level crossing and optical pumping

**QICS.** 15.10.Ph Photons

## 1 Introduction

Since the initial prediction of photonic crystal by Yablonovitch and John [1], photonic crystals have attracted much attention and become an intensive research area. Photonic crystals are periodically modulated dielectric structures with the existence of one or several complete photonic band gaps (PBG). A photonic band gap is a frequency interval within which no propagating electromagnetic (EM) modes are allowed and the propagation of electromagnetic (EM) waves is forbidden in all directions. The dispersion characteristics of radiation waves traveling in a photonic crystal are changed, and the mode density of the electromagnetic field is strongly different from that of the free space vacuum field. Consequently, photonic crystals lead to a new frontier in quantum optics and offer many new technological applications.

Spontaneous emission is a fundamental concept in atomic physics. It is well-known that spontaneous emission is the result from the coupling of the atoms or molecules to the vacuum modes of the electromagnetic field, and depends not only on the properties of the excited atomic system but also on the nature of the surrounding environment, specifically on the density of electromagnetic vacuum modes [2]. Furthermore, to control spontaneous emission well is important for the control of an atom in terms of its stability. If the excited atoms are embedded in photonic crystals, the relation between the atomic dynamic properties and the time decay of the radiation may be changed due to the influence of the special surrounding environment. So the change of mode density and the inhibition of electromagnetic wave propagation in photonic crystals provide a way to control the spontaneous emission, which would promote the development of optics and optoelectronics, and has many important applications [3]. During recent years, considerable attention has been paid to the properties of spontaneous emission from an initially excited atom embedded in photonic crystals [4–21]. The previous studies show that the gap edge has great influence on the optical behavior of an atom in a photonic crystal, and many interesting effects have been discovered when the atomic resonant transition frequencies are near the photonic band edge, such as localization of light [1,4], non-exponential spontaneous decay [5], spectral splitting [5,7], the formation of photon-atom bound states [5–10], suppression and even complete cancellation of spontaneous emission [8,9], periodic and quasiperiodic oscillations, the enhancement of spontaneous emission interference [7,10], coherent control of spontaneous emission [11], the occurrence of dark lines in spontaneous emission [12], accelerated and decelerated decays of the radiation from an atom [13], the quantum Zeno effect and the quantum anti-Zeno effect [14], the creation of

[a] e-mail: xieshy@hotmail.com
or xieshuangyuan@mail.tongji.edu.cn

entanglement [15], giant Lamb shift in photonic crystals [16], the quantum features of one-atom laser emission in photonic crystals [17], the optical switching effect and the mechanism of controlling light with light [18], discussion about the low frequency field influence on spontaneous emission [19], the experimental observation of directional spontaneous emission spectra [20], the control of spontaneous emission rate of single quantum dots [21], etc.

On the other hand, coherent interaction of atom with external driving field can have a profound effect on radiative dynamic of the atom, which is one of the basic research field in quantum optics. With the external driving field, the atomic system can lead to many interesting quantum phenomena: electromagnetically induced transparency (EIT) [22], the collapse and revival of the atomic population [23], population inversion without emission [24], lasing without population inversion [25], a dark line in the spontaneous emission spectrum [26], etc. The emission spectrum for a ladder three-level atomic system with external driving field was studied by Zhu in reference [26], and the dark line, non-Lorentzian shape are found in the emission spectrum due to quantum interference. The emission spectrum for a ladder three-level atomic system without external driving field in a photonic crystal was studied by Bay and Lambropoulos in reference [6]. The coherent control of spontaneous emission from a $\Lambda$ or $V$ three-level system was discussed in reference [11], which is based on the isotropic photonic crystal. However, in these studies, an isotropic photonic dispersion relation was used in order to simplify the calculation, which results in a singularity for the density of states at the band edge. If the vector nature of electromagnetic waves can be neglected or the mode structures of the photonic crystal are same in all spatial directions, the isotropic model is a good approximation and leads to qualitatively correct physics and exhibits many of the observed and computed features of 3D PBG structures. If the mode structures of the photonic crystals are different in different spatial directions, a three-dimensional anisotropic photonic dispersion relation should be adopted to model the band edge of photonic crystals, where the singularity of the density of states is removed. From our earlier studies, it is found that the anisotropic model indeed leads to rather unusual phenomena as comparing with the isotropic case. For example: the disappearance of localized field, no quasi-oscillation for the population evolution, no coexistence of the localized field and the propagating field, the enhancement of the diffusion field [10,27,28], etc. Not only the external driving field, but also the special environment anisotropic photonic crystal can play important roles in the interaction between light and materials and can affect the properties of the spontaneous emission from an excited atom.

In the present paper, we investigate the spontaneous radiation from a ladder three-level atom embedded in a three-dimensional anisotropic photonic crystal with an external driving field. The properties of the spontaneous emission are dependent strongly on the relative position of the middle level from the band edge. Due to the Autler-Townes splitting by the action of the driving field, the external driving field can also affect the properties of the spontaneous emission. The population exchanged between the upper and the middle levels decreases as the detuning of the external driving field frequency from the corresponding transition frequency increases. The properties of the emission field can be changed or so much as controlled by choosing suitable intensity of the external driving field. The emission spectrum is more complex, and dependent on the location of the observer in this case.

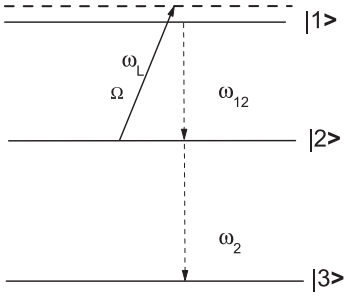


**Fig. 1.** The scheme of the ladder three-level atom in this system.

This paper is organized as follows. In Section 2, the model and the basic theory to study the spontaneous emission are given. The properties of the time evolution of the population trapped in the excited state are discussed in Section 3. In Section 4, we investigate the properties of the emitted field in detail. In Section 5, we pay attention to the spontaneous emission spectra of the system.

## 2 Basic theory

We consider a three-level atom in a cascade configuration, with atomic levels $|1\rangle$, $|2\rangle$, $|3\rangle$ and eigenenergies $\hbar\omega_1$, $\hbar\omega_2$, 0 respectively, where $\omega_1 > \omega_2$ (as shown in Fig. 1) embedded in a three-dimensional anisotropic photonic crystal. The upper level $|1\rangle$ is coupled by an external driving field to the middle level $|2\rangle$, which is coupled by vacuum modes to the lower level $|3\rangle$. The resonant frequency between levels $|2\rangle$ and $|3\rangle$ is $\omega_2$, which is assumed to be near the edge of a photonic band gap. Performing the rotating wave approximation (RWA) for the interaction, the Hamiltonian of this system takes the form

$$\begin{aligned} H = {} & \hbar\omega_1 |1\rangle\langle 1| + \hbar\omega_2 |2\rangle\langle 2| + \sum_k \hbar\omega_k b_k^\dagger b_k \\ & + i\hbar \sum_k g_k (b_k^\dagger |3\rangle\langle 2| - b_k |2\rangle\langle 3|) \\ & + i\hbar\Omega (e^{i\omega_L t} |2\rangle\langle 1| - e^{-i\omega_L t} |1\rangle\langle 2|), \end{aligned} \quad (1)$$

where $b_k$ ($b_k^\dagger$) is the annihilation (creation) operator for the $k$th reservoir mode with frequency $\omega_k$. $g_k$ is the coupling constant between the atomic transition $|2\rangle \longrightarrow |3\rangle$ and the $k$th electromagnetic mode. It is well-known that the mode functions in a whole photonic crystal are Bloch functions. Since we are concerned here with a model very close to the edge of the band gap, we use the free-space

mode functions instead of the Bloch functions in the following discussions. It is expected to be a good approximation for large gaps, and for atomic transition frequencies close to the edge of the band gap. For the model near the band edge, the coupling constant $g_k$ can be approximated by $g_k = \omega_2 d_2/\hbar\sqrt{\hbar/(2\varepsilon_0\omega_k V_0)}\mathbf{e}_k \cdot \mathbf{u}_d$. $k$ represents both the momentum and polarization of the modes. $d_2$ and $\mathbf{u}_d$ are the magnitude and unit vector of the atomic dipole moment of the transition, $V_0$ is the quantization volume, $\mathbf{e}_k$ are the transverse unit vectors for the reservoir modes, and $\varepsilon_0$ is the Coulomb constant. $\Omega$ and $\omega_L$ represent the intensity and frequency of the external driving field. If a three-dimensional anisotropic photonic crystal has an allowed point-group symmetry, the dispersion relation near the band edge could be expressed approximately by

$$\omega_k = \omega_c + A|\mathbf{k} - \mathbf{k}_0^j|^2, \quad (\omega_k > \omega_c), \tag{2}$$

where $\omega_c$ is the cut-off frequency of the band edge. $\mathbf{k}_0^j$ are the finite collections of symmetry related points, which are associated with the band edge. $A$ is the model-dependent constant.

We assume the atom initially in the middle level $|2\rangle$, and the radiation field is in the vacuum state. The wave function of the system at arbitrary time $t$ may be written as

$$|\psi(t)\rangle = A_1(t)e^{-i\omega_1 t}|1,\{0\}\rangle + A_2(t)e^{-i\omega_2 t}|2,\{0\}\rangle + \sum_k B_k(t)e^{-i\omega_k t}|3,\{1_k\}\rangle \tag{3}$$

with $A_1(0) = B_k(0) = 0$, $A_2(0) = 1$. The state vector $|1,\{0\}\rangle$ ($|2,\{0\}\rangle$) describes the atom in its excited state $|1\rangle$ ($|2\rangle$) with no photons in all reservoir modes, and the state vector $|3,\{1_k\}\rangle$ represents the atom in its ground state $|3\rangle$ and a single photon in $k$th mode with frequency $\omega_k$. From the Schrödinger equation $i\hbar\frac{\partial}{\partial t}|\psi(t)\rangle = H|\psi(t)\rangle$, we can obtain the following first-order differential equations for the amplitudes $A_1(t)$, $A_2(t)$ and $B_k(t)$,

$$\frac{\partial}{\partial t}A_1(t) = -\Omega A_2(t)e^{-i\omega_{L12}t}, \tag{4a}$$

$$\frac{\partial}{\partial t}A_2(t) = \Omega A_1(t)e^{i\omega_{L12}t} - \sum_k g_k B_k(t)e^{-i\omega_{k2}t}, \tag{4b}$$

$$\frac{\partial}{\partial t}B_k(t) = g_k A_2(t)e^{i\omega_{k2}t} \tag{4c}$$

where we assume: $\omega_{L12} = \omega_L - \omega_1 + \omega_2$, $\omega_{k2} = \omega_k - \omega_2$.

Formally integrating the equation (4c), and then substituting into equation (4b), we have

$$\frac{\partial}{\partial t}A_2(t) = -\sum_k g_k^2 \int_0^t A_2(t')e^{-i\omega_{k2}(t-t')}dt' + \Omega A_1(t)e^{i\omega_{L12}t}. \tag{5}$$

With the help of the Laplace transform, we can solve the above equations. The Laplace transform $A_1(s)$ and $A_2(s)$ for the amplitudes $A_1(t)$ and $A_2(t)$ are found as

$$A_1(s - i\omega_{L12}) = \frac{A_1(0)[s + \Gamma(s)] - \Omega A_2(0)}{[s + \Gamma(s)](s - i\omega_{L12}) + \Omega^2}, \tag{6a}$$

$$A_2(s) = \frac{A_2(0)(s - i\omega_{L12}) + \Omega A_1(0)}{[s + \Gamma(s)](s - i\omega_{L12}) + \Omega^2}. \tag{6b}$$

Where

$$\Gamma(s) = \sum_k g_k^2/[s + i(\omega_k - \omega_2)] = -i\beta^{3/2}/[\sqrt{\omega_c} + \sqrt{-is - (\omega_2 - \omega_c)}],$$

with $\beta^{3/2} = (\omega_2 d_2)^2 \sum_j \sin^2\theta_j/(8\pi\epsilon_0\hbar A^{3/2})$ (see Appendix A) and $\omega_{2c} = \omega_2 - \omega_c$. Here $\theta_j$ is the angle between the dipole vector of the atom and the $j$th $\mathbf{k}_0^j$. The phase angle of $s$ is defined by $-\pi < \arg(s) < \pi$, and the phase angle of $\sqrt{-is - (\omega_2 - \omega_c)}$ is defined by $-\frac{\pi}{2} < \arg(\sqrt{-is - (\omega_2 - \omega_c)}) < \frac{\pi}{2}$.

The amplitudes $A_1(t)$ and $A_2(t)$ can then be obtained by means of the inverse Laplace transform

$$A_1(t) = \frac{1}{2\pi i}\int_{\sigma-i\infty}^{\sigma+i\infty} A_1(s)e^{st}ds, \tag{7a}$$

$$A_2(t) = \frac{1}{2\pi i}\int_{\sigma-i\infty}^{\sigma+i\infty} A_2(s)e^{st}ds, \tag{7b}$$

where the real number $\sigma$ is chosen so that $s = \sigma$ lies to the right of all the singularities (poles and branch points) of the functions $A_1(s)$ and $A_2(s)$. With the help of complex function integration and the residue theorem, we can obtain the expression of the amplitudes (see Appendix B):

$$A_1(t) = e^{-i\omega_{L12}t}\left[\sum_j \frac{f_2(x_j^{(1)})}{G'(x_j^{(1)})}e^{x_j^{(1)}\beta t} + \sum_j \frac{f_3(x_j^{(2)})}{H'(x_j^{(2)})}e^{x_j^{(2)}\beta t} + \frac{e^{i\omega_{2c}t}}{\pi}\int_0^\infty \frac{f_6(x)}{f_4(x)}e^{-x\beta t}dx\right], \tag{8a}$$

$$A_2(t) = \sum_j \frac{f_1(x_j^{(1)})}{G'(x_j^{(1)})}e^{x_j^{(1)}\beta t} + \sum_j \frac{f_1(x_j^{(2)})}{H'(x_j^{(2)})}e^{x_j^{(2)}\beta t} + \frac{e^{i\omega_{2c}t}}{\pi}\int_0^\infty \frac{f_5(x)}{f_4(x)}e^{-x\beta t}dx. \tag{8b}$$

where these functions $f_1(x)$, $f_2(x)$, $f_3(x)$, $f_4(x)$, $f_5(x)$, $f_6(x)$, $G(x)$, and $H(x)$ are defined in Appendix B. $x_j^{(1)}$ are the roots of the equation $G(x) = 0$ in region [$\mathrm{Re}(x) > 0$] or [$\mathrm{Im}(x) > \omega_{2c}$], and $x_j^{(2)}$ are the roots of the equation $H(x) = 0$ in region [$\mathrm{Re}(x) < 0$ and $\mathrm{Im}(x) < \omega_{2c}$]. $G'(x)$ and $H'(x)$ are the derivatives of those functions $G(x)$ and $H(x)$, respectively. With the help of numerical calculation, we found that there are at least one root and at

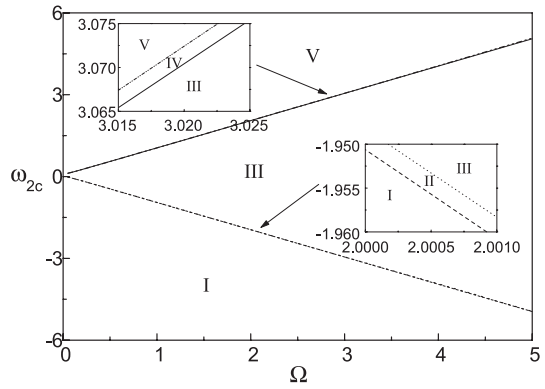


**Fig. 2.** Five-region distribution for roots with $\omega_c = 100\beta$ and $\omega_{L12} = 0$.

most two roots. We can classify these roots into two types: (i) pure imaginary root $x_j^{(1)}$ with its imaginary part larger than $\omega_{2c}$; (ii) complex root $x_j^{(2)}$ with a negative real part and an imaginary part smaller than $\omega_{2c}$. The number and characteristics of these roots are dependent on the driving field and the relative position of the middle level $|2\rangle$ of the atom from the band edge. For example, we have five regions in the space of ($\omega_{2c}$,$\Omega$) with $\omega_c = 100\beta$, $\omega_{L12} = 0$ (as shown in Fig. 2) according to the number and the values of the roots. There are two pure imaginary roots in region I, only one pure imaginary root in region II, one complex root and one pure imaginary root in region III, only one complex root in region IV, two complex roots in region V. The last term in the right of equations (8a, 8b) comes from the single-valued branch point contribution. From the expressions of the amplitudes $A_1(t)$ and $A_2(t)$, we can see that these roots are important in study of the dynamical properties of the excited atom.

The amplitude of the radiation field at a particular space point $\mathbf{r}$ can be calculated from $B_k(t)$ via $A_2(t)$ in the standard way (see Appendix C) [29]:

$$\mathbf{E}(\mathbf{r},t) = \sum_k \sqrt{\frac{\hbar\omega_k}{2\varepsilon_0 V_0}} e^{-i(\omega t - \mathbf{k}\cdot\mathbf{r})} B_k(t)\mathbf{e}_k. \tag{9}$$

The emission spectrum $\mathbf{S}(\mathbf{r},\boldsymbol{\omega})$ can be obtained by using the Fourier transform of the radiation field (see Appendix D),

$$\mathbf{S}(\mathbf{r},\boldsymbol{\omega}) = |\mathbf{F}(\mathbf{r},\boldsymbol{\omega})|^2 \tag{10}$$

with $\mathbf{F}(\mathbf{r},\boldsymbol{\omega}) = (\mathbf{1}/2\pi)\int_0^\infty \mathbf{E}(\mathbf{r},t)e^{i\omega t}dt$.

## 3 Spontaneous emission

The influence of the external driving field on the spontaneous decay from the excited atom can be investigated by examining the time evolution of the population in the upper level $|1\rangle$ and the middle level $|2\rangle$, which can be obtained from equations (8a, 8b):

$$P_1(t) = |A_1(t)|^2, \tag{11a}$$

$$P_2(t) = |A_2(t)|^2 \tag{11b}$$

and the total population is

$$P(t) = |A_1(t)|^2 + |A_2(t)|^2. \tag{12}$$

The first term in the right of equations (8a, 8b) comes from the pure imaginary roots $x_j^{(1)} = ib_j^{(1)}/\beta$ with $\omega_2 - b_j^{(1)} < \omega_c$ corresponding to photon-atom bound dressed states caused by the interaction between the atom and its own radiation occur at frequencies $\omega_2 - b_j^{(1)}$, which are within the band gap and without decay. The dressed states without decay lead to a fractionalized steady-state population trapped in the upper level. While the second term in the right of equations (8a, 8b) comes from complex roots $x_j^{(2)} = (a_j^{(2)} + ib_j^{(2)})/\beta$ with $\omega_2 - b_j^{(2)} > \omega_c$ and $a_j^{(2)} < 0$ corresponding to photon-atom bound dressed states occur at frequencies $\omega_2 - b_j^{(2)}$, which are within the traveling band and the excited states population decay. The last term in the right of equations (8a, 8b) yields a quasidressed state at the band-edge frequency $\omega_c$. The quasidressed state displays behavior of power-law decay, and a fractionalized population in the excited states decays to the ground state $|3\rangle$. It is easy to see that these dressed states and quasidressed states are the combined results of the effect of the band edge and the Autler-Townes splitting by the external field.

The properties of the excited atomic population decay are dependent on the relative position of the middle level $|2\rangle$ from the band edge. When the middle level $|2\rangle$ is in region I, we have two pure imaginary roots. The first and last terms in the right of equations (8a) and (8b) exist, and other terms are replaced by zero. Due to the Rabi oscillation the populations in the levels $|1\rangle$ and $|2\rangle$ display oscillatory periodic behavior for large time $t$ (see Fig. 3a), which represents the transfer of population between levels $|1\rangle$ and $|2\rangle$ always exists. As the middle level $|2\rangle$ is in region I (III, V) the amplitude of the quasidressed state is negligibly small compared to the atomic dressed state. When the middle level $|2\rangle$ is in region II, we have only one pure imaginary root. The first and last terms in the right of equations (8a) and (8b) exist, and the second term is replaced by zero. In this region, the decay corresponding to the quasidressed state is too strong to be ignored. The Rabi oscillation leads to quasi-oscillatory behavior of the population and the existence of the quasidressed state leads to only a fractionally fractionalized population in the excited states decays to the ground state $|3\rangle$ for large time $t$ (see Fig. 3b). When the middle level $|2\rangle$ is in region III, we have one pure imaginary root and one complex root. All terms in the right of equations (8a) and (8b) exist. As a result of the Rabi oscillation, the population displays the quasi-oscillatory behavior. The decaying dressed state leads to a fractionalized population in the excited states decay to the ground state $|3\rangle$ for large time $t$ (see Fig. 3c). Comparing Figure 3b with Figure 3c, we found that the decay of the population in Figure 3b is slower than that in Figure 3c. The reason is that the quasidressed state decays in the manner of a power-law decay, while the dressed state corresponding complex root displays behavior of exponential decay. When the middle level $|2\rangle$ is in

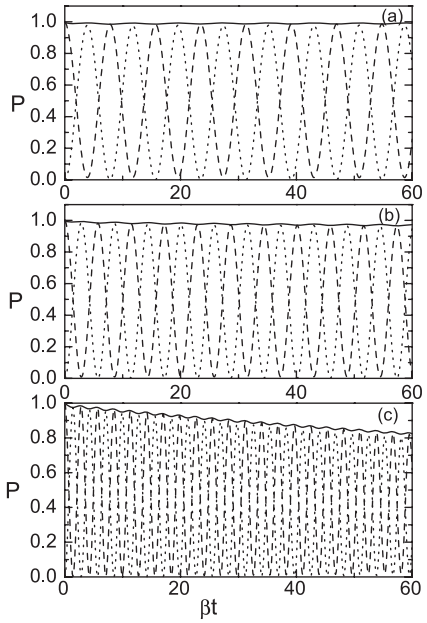


**Fig. 3.** The excited state population $P(t)$ (solid curve), $P_1(t)$ (dotted curve), $P_2(t)$ (dashed curve) as a function of the scaled time $\beta t$ for $\omega_c = 100\beta$, $\omega_{L12} = 0$, $\omega_{2c} = -0.5\beta$, and different Rabi frequency of the external driving field. (a) $\Omega = 0.4\beta$ (region I); (b) $\Omega = 0.547725\beta$ (region II); (c) $\Omega = 1.1\beta$ (region III).

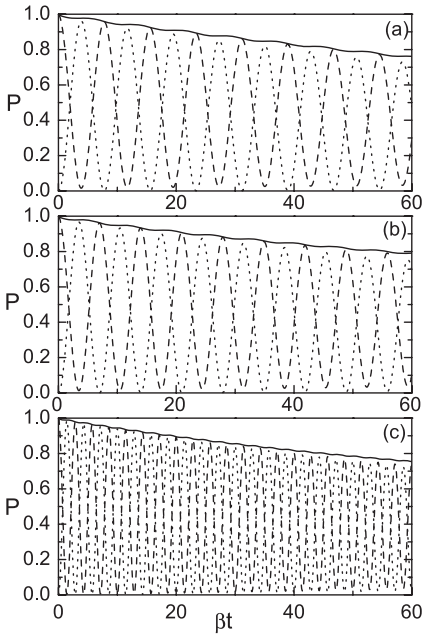


**Fig. 4.** The excited state population $P(t)$ (solid curve), $P_1(t)$ (dotted curve), $P_2(t)$ (dashed curve) as a function of the scaled time $\beta t$ for $\omega_c = 100\beta$, $\omega_{L12} = 0$, $\omega_{2c} = 0.5\beta$, and different Rabi frequency of the external driving field. (a) $\Omega = 0.4\beta$ (region V); (b) $\Omega = 0.447205\beta$ (region IV); (c) $\Omega = 1.1\beta$ (region III).

region IV, we have only one complex root. The second and last terms in the right of equations (8a) and (8b) remain, and the first term is replaced by zero. Similarity to region II, the decay corresponding to the quasidressed state is too strong to be ignored in this region. The population displays the quasi-oscillatory behavior because of the Rabi oscillation and the population in the excited states can decay to zero as time goes to infinity (see Fig. 4b) because of the disappearance of the non-decaying dressed sate. As the middle level $|2\rangle$ is in region V, we have two complex roots. The second and last terms in the right of equations (8a) and (8b) remain. The Rabi oscillation leads to quasi-oscillatory behavior of the population and the population in the excited states can decay to zero faster than that in region IV (see Fig. 4a).

The properties of the excited atomic population decay also depend on the driving field. If the intensity of the driving field $\Omega$ is zero, the problem is reduced to a two-level atom problem already treated in reference [28]. In this case, we know that the spontaneous emission field dresses the atom to form a dressed state, and the properties of the dressed state are dependent on the nature of the emission field. The excited state population can display non-decay (an exponentially decay, a power law decay) corresponding to the emission field is localized field (propagating field, diffusion field). The emission field is essentially composed of only one field at one time. Therefore, the excited state population will have no quasi-oscillation because of the lack of Rabi oscillation. From the above discussion, we can see clearly that the population of the middle level $|2\rangle$ can display non-decaying oscillatory periodic behavior or quasi-oscillatory decay with the driving field between the levels $|1\rangle$ and $|2\rangle$. The excited state corresponding to the middle level $|2\rangle$ is split into Autler-Townes doublets by the action of the driving field. Further more, the Autler-Townes doublets can form dressed states (due to the strong interaction between the atom and its own radiation field) in a combinating fashion due to the interference between the two transitions from the Autler-Townes doublets to the lower level. Therefore, the dressed states are the combined results under the action of the driving field and the photonic crystal. In Figures 3 and 4 we plot the time evolution of the excited states population with $\omega_c = 100\beta$, and $\omega_{L12} = 0$ for fixed relative positions of the middle level $|2\rangle$ but different $\Omega$: $\omega_2 = 99.5\beta$, $\Omega = 0.4\beta$ (region I), $\Omega = 0.547725\beta$ (region II), $\Omega = 1.1$ (region III) for Figure 3 and $\omega_2 = 100.5\beta$, $\Omega = 0.4$ (region V), $\Omega = 0.447205\beta$ (region IV), $\Omega = 1.1\beta$ (region III) for Figure 4. From Figure 3, it is found that if the middle level $|2\rangle$ is within the band gap initially, the two dressed states are still within the band gap for weak driving field, while one dressed state goes into deep band gap and the other dressed state can move into the traveling band with a stronger driving field. On the contrary, if the middle level $|2\rangle$ is within the traveling band initially, the two dressed states are still within the traveling band for weak driving field, while one dressed state goes deeply into the traveling band and the other dressed state can move into the band gap with a stronger driving field as shown in Figure 4. These phenomena can also be rationalized in a somewhat different language more familiar in quantum optics. Due to the strong external driving field, one of the

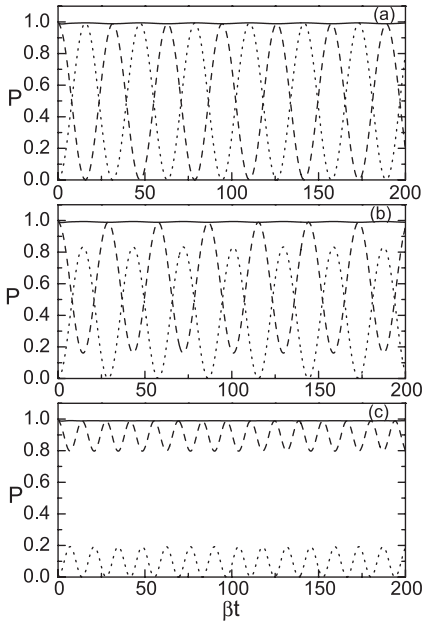


**Fig. 5.** The excited state population $P(t)$ (solid curve), $P_1(t)$ (dotted curve), $P_2(t)$ (dashed curve) as a function of the scaled time $\beta t$ for $\omega_c = 100\beta$, $\Omega = 0.1\beta$, $\omega_{2c} = -0.5\beta$, and different detuning from the transition frequency $\omega_{12}$: (a) $\omega_{L12} = 0$; (b) $\omega_{L12} = 0.005\beta$; (c) $\omega_{L12} = 0.5\beta$.

two components created by the Autler-Townes splitting is pushed into the band gap, where it is protected against decay, while the other is pushed into the traveling band where it can decay.

On the other hand, the detuning of the external driving field frequency from the transition frequency $\omega_{12}$ can also affect the time evolution of the populations in the levels $|1\rangle$ and $|2\rangle$. In Figure 5 we plot the time evolution of the populations in the excited states with $\omega_c = 100\beta$, $\Omega = 0.1\beta$, $\omega_{2c} = -0.5\beta$, but for different detuning $\omega_{L12}$. Here we just focus on the case corresponding to the middle level $|2\rangle$ in region I in Figure 2. When the middle level $|2\rangle$ is in region I, there are two dressed states without decay. The oscillatory periodic behavior of the populations in the levels $|1\rangle$ and $|2\rangle$ indicates that the population is exchanged between levels $|1\rangle$ and $|2\rangle$ with the help of the external driving field. Moreover, almost no population decays to the lower level $|3\rangle$ due to the middle level $|2\rangle$ in region I and the transition from level $|2\rangle$ to lower level $|3\rangle$ is forbidden. From Figure 5, we can see that the detuning $\omega_{L12}$ determines what fraction of the population is exchanged between levels $|1\rangle$ and $|2\rangle$. When the external driving field is resonant with or detuned near the transition $|1\rangle \leftrightarrow |2\rangle$, it is easy for the population to exchange and the amplitude of the exchanging population is large. On the contrary, when the driving field is detuned away from the transition frequency $\omega_{12}$, the amplitude becomes small because the exchange of the population is difficult in this case. Moreover, the frequency of the oscillatory periodic behavior of the population increases as the detuning increases.

## 4 The emitted field

From equations (8b) and (9) we can calculate the emission field under the approximation $\mathbf{k}\cdot\mathbf{r} \gg 1$ [29]. Corresponding to three terms of equation (8b) the radiated field can be written as the sum of three parts,

$$\mathbf{E}(\mathbf{r},t) = \mathbf{E}^{(1)}(\mathbf{r},t) + \mathbf{E}^{(2)}(\mathbf{r},t) + \mathbf{E}^{(3)}(\mathbf{r},t). \tag{13}$$

$\mathbf{E}^{(1)}(\mathbf{r},t)$ comes from the pure imaginary root $x^{(1)}$, and $\mathbf{E}^{(2)}(\mathbf{r},t)$ stems from the complex root $x^{(2)}$. $\mathbf{E}^{(3)}(\mathbf{r},t)$ comes from the last term (the power-law-decay term) in equation (8b).

When the middle level $|2\rangle$ is within region I, we have two pure imaginary roots $x_1^{(1)} = ib_1^{(1)}/\beta$, $x_2^{(1)} = ib_2^{(1)}/\beta$ and $\mathbf{E}(\mathbf{r},t) = \mathbf{E}^{(1)}(\mathbf{r},t) + \mathbf{E}^{(3)}(\mathbf{r},t)$. From equations (C.7) and (C.9) we can rewrite the emission field $\mathbf{E}(\mathbf{r},t)$ as follows,

$$\mathbf{E}(\mathbf{r},t) = \mathbf{E}_{l1}^{(1)}(\mathbf{r},t)+\mathbf{E}_{l2}^{(1)}(\mathbf{r},t)+\mathbf{E}_{d1}(\mathbf{r},t)+\mathbf{E}_{d2}^{(1)}(\mathbf{r},t) \tag{14}$$

with

$$\mathbf{E}_{lj}^{(1)}(\mathbf{r},t) = \mathbf{E}_0(\mathbf{r})\frac{f_1(x_j^{(1)})}{G'(x_j^{(1)})}\frac{\pi}{A}e^{-i(\omega_2-b_j^{(1)})t-r/l_j}\Theta\left(t-\frac{r}{v_{fj}^{(1)}}\right),$$

$$\mathbf{E}_{d1}(\mathbf{r},t) = \mathbf{E}^{(3)}(\mathbf{r},t),$$

$$\mathbf{E}_{d2}^{(1)}(\mathbf{r},t) = \mathbf{E}_0(\mathbf{r})e^{\phi}\left[\frac{f_1(x_1^{(1)})}{G'(x_1^{(1)})}J(r,t,x_1^{(1)}) + \frac{f_1(x_2^{(1)})}{G'(x_2^{(1)})}J(r,t,x_2^{(1)})\right],$$

$$\mathbf{E}_0(\mathbf{r}) = \frac{\omega_2 d_2}{8\pi^2\varepsilon_0 ri}\sum_j e^{i\mathbf{k}_0^j\cdot\mathbf{r}}\left[\mathbf{u}_d - \frac{\mathbf{k}_0^j(\mathbf{k}_0^j\cdot\mathbf{u}_d)}{(k_0^j)^2}\right],$$

$$J(r,t,x) = \int_{-\infty}^{\infty}\frac{(\rho e^{\frac{3}{4}\pi i}+\frac{r}{2At})e^{-At\rho^2}}{(\omega_c-\omega_2-ix\beta)+A(\rho e^{\frac{3}{4}\pi i}+\frac{r}{2At})^2}d\rho,$$

where $\phi = -i(\omega_c t - \frac{r^2}{4At}) + \frac{1}{4}\pi i$, $\Theta(x)$ is the Heaviside step function. The frequency of the fields $\mathbf{E}_{l1}^{(1)}(\mathbf{r},t)$ ($\mathbf{E}_{l2}^{(1)}(\mathbf{r},t)$) is $\omega_2 - b_1^{(1)}$ ($\omega_2 - b_2^{(1)}$), which is within the band gap. Obviously, these two fields represent localized fields without decay in time. The amplitudes of the localized fields $\mathbf{E}_{l1}^{(1)}(\mathbf{r},t)$ and $\mathbf{E}_{l2}^{(1)}(\mathbf{r},t)$ drop exponentially with increasing distance from the atom as $e^{-r/l_1}$ and $e^{-r/l_2}$, respectively. The localization lengths are $l_1 = \sqrt{A/(\omega_c-\omega_2+b_1^{(1)})}$ and $l_2 = \sqrt{A/(\omega_c-\omega_2+b_2^{(1)})}$, and the front velocities of the localized fields are $v_{f1}^{(1)} = 2\sqrt{A(\omega_c-\omega_2+b_1^{(1)})}$ and $v_{f2}^{(1)} = 2\sqrt{A(\omega_c-\omega_2+b_2^{(1)})}$. The localized fields $\mathbf{E}_{l1}^{(1)}(\mathbf{r},t)$ and $\mathbf{E}_{l2}^{(1)}(\mathbf{r},t)$ do not decay against time and their distributions with their energy are trapped in the vicinity of the atom. That is, the corresponding dressed state is the photon-atom bound dressed state with no decay. A photon which is emitted by the atom in this dressed state

will tunneling on a length scale given by the localization length before Bragg reflected back to the emitting atom. This photon-atom bound state leads to the fractionalized steady-state atomic population in the excited state. $\mathbf{E}_{d1}(\mathbf{r},t)$ and $\mathbf{E}^{(1)}_{d2}(\mathbf{r},t)$ are the diffusion fields, which have power-law decay and are without fixed phase difference between two space points. The expression of $\mathbf{E}_{d1}(\mathbf{r},t)$ is given in equation (C.9), which comes from the branch-point contribution, while $\mathbf{E}^{(1)}_{d2}(\mathbf{r},t)$ comes from the first term $\sum_j f_1(x_j^{(1)})e^{x_j^{(1)}t}/G'(x_j^{(1)})$ in equation (8b).

When the middle level $|2\rangle$ gets into region V, we have two complex roots $x_j^{(2)} = (a_j^{(2)} + ib_j^{(2)})/\beta$, $(j = 1, 2)$. The radiation field $\mathbf{E}(\mathbf{r},t)$= $\mathbf{E}^{(2)}(\mathbf{r},t) + \mathbf{E}^{(3)}(\mathbf{r},t)$ and can be rewritten as (see Eqs. (C.8) and (C.9))

$$\mathbf{E}(\mathbf{r},t) = \mathbf{E}^{(2)}_{p1}(\mathbf{r},t)+\mathbf{E}^{(2)}_{p2}(\mathbf{r},t)+\mathbf{E}_{d1}(\mathbf{r},t)+\mathbf{E}^{(2)}_{d2}(\mathbf{r},t) \quad (15)$$

with

$$\mathbf{E}^{(2)}_{pj}(\mathbf{r},t) = \mathbf{E}_0(\mathbf{r})\frac{f_1(x_j^{(2)})}{H'(x_j^{(2)})}\frac{\pi}{A} \times e^{-i(\omega_2-b_j^{(2)})(t-r/v_{pj}^{(2)})+a_j^{(2)}(t-r/v_{ej}^{(2)})}\Theta\left(t-\frac{r}{v_{fj}^{(2)}}\right),$$

$$\mathbf{E}_{d1}(\mathbf{r},t) = \mathbf{E}^{(3)}(\mathbf{r},t),$$

$$\mathbf{E}^{(2)}_{d2}(\mathbf{r},t) = \mathbf{E}_0(\mathbf{r})e^{\phi}\left[\frac{f_1(x_1^{(2)})}{H'(x_1^{(2)})}J(r,t,x_1^{(2)}) + \frac{f_1(x_2^{(2)})}{H'(x_2^{(2)})}J(r,t,x_2^{(2)})\right].$$

The frequency of $\mathbf{E}^{(2)}_{pj}(\mathbf{r},t)$ is $\omega_2 - b_j^{(2)}$, $(j = 1, 2)$, which is within the traveling band. $\mathbf{E}^{(2)}_{pj}(\mathbf{r},t)$ represents a propagating field, which can travel away coherently from the atom in the form of a traveling pulse with phase velocity $v_{pj}^{(2)} = (\omega_2 - b_j^{(2)})\sqrt{A}/\mathrm{Im}(\sqrt{\omega_2-\omega_c+ix_j^{(2)}\beta})$ and the energy velocity $v_{ej}^{(2)} = -a_j^{(2)}\sqrt{A}/\mathrm{Re}(\sqrt{\omega_2-\omega_c+ix_j^{(2)}\beta})$. The front velocity of the propagating field is $v_{fj}^{(2)} = 2\sqrt{A}(\mathrm{Re} - \mathrm{Im})\sqrt{\omega_c-\omega_2-ix_j^{(2)}\beta}$, $(j = 1, 2)$. $\mathbf{E}_{d1}(\mathbf{r},t)$ and $\mathbf{E}^{(2)}_{d2}(\mathbf{r},t)$, which comes from the second term $\sum_j \frac{f_1(x_j^{(2)})}{H'(x_j^{(2)})}e^{x_j^{(2)}t}$ in equation (8b), represent the diffusion fields.

Similarly, when the middle level $|2\rangle$ gets into region III, we can obtain one pure imaginary root $x^{(1)} = ib^{(1)}/\beta$ and one complex root $x^{(2)} = (a^{(2)} + ib^{(2)})/\beta$. The radiation field $\mathbf{E}(\mathbf{r},t)$ =$\mathbf{E}^{(1)}(\mathbf{r},t)$+$\mathbf{E}^{(2)}(\mathbf{r},t)$+$\mathbf{E}^{(3)}(\mathbf{r},t)$ and can be rewritten as (see Eqs. (C.7), (C.8), and (C.9))

$$\mathbf{E}(\mathbf{r},t) =\mathbf{E}^{(1)}_{l}(\mathbf{r},t)+\mathbf{E}^{(2)}_{p}(\mathbf{r},t)+\mathbf{E}_{d1}(\mathbf{r},t)+\mathbf{E}_{d2}(\mathbf{r},t), \quad (16)$$

with

$$\mathbf{E}^{(1)}_{l}(\mathbf{r},t) = \mathbf{E}_0(\mathbf{r})\frac{f_1(x^{(1)})}{G'(x^{(1)})}\frac{\pi}{A}e^{-i(\omega_2-b^{(1)})t-r/l}\Theta\left(t-\frac{r}{v_f^{(1)}}\right),$$

$$\mathbf{E}^{(2)}_{p}(\mathbf{r},t) = \mathbf{E}_0(\mathbf{r})\frac{f_1(x^{(2)})}{H'(x^{(2)})}\frac{\pi}{A} \times e^{-i(\omega_2-b^{(2)})(t-r/v_p^{(2)})+a_j^{(2)}(t-r/v_e^{(2)})}\Theta\left(t-\frac{r}{v_f^{(2)}}\right),$$

$$\mathbf{E}_{d1}(\mathbf{r},t) = \mathbf{E}^{(3)}(\mathbf{r},t),$$

$$\mathbf{E}_{d2}(\mathbf{r},t) = \mathbf{E}_0(\mathbf{r})e^{\phi}\left[\frac{f_1(x^{(1)})}{G'(x^{(1)})}J(r,t,x^{(1)}) + \frac{f_1(x^{(2)})}{H'(x^{(2)})}J(r,t,x^{(2)})\right].$$

The field $\mathbf{E}^{(1)}_{l}(\mathbf{r},t)$ represents a localized field without decay in time due to its frequency is $\omega_2 - b^{(1)} < \omega_c$, which is within the band gap. The frequency of field $\mathbf{E}^{(2)}_{p}(\mathbf{r},t)$ is $\omega_2 - b^{(2)} > \omega_c$, which is within the traveling band and the field $\mathbf{E}^{(2)}_{p}(\mathbf{r},t)$ is a propagating field. $\mathbf{E}_{d1}(\mathbf{r},t)$ and $\mathbf{E}_{d2}(\mathbf{r},t)$ are the diffusion fields. $\mathbf{E}_{d2}(\mathbf{r},t)$ comes from these terms $\frac{f_1(x^{(1)})}{G'(x^{(1)})}e^{x^{(1)}t}$ and $\frac{f_1(x^{(2)})}{H'(x^{(2)})}e^{x^{(2)}t}$ in equation (8b).

As the middle level $|2\rangle$ is in regions II or IV, there is only one pure imaginary or complex root exists. The emitted field can be rewritten as

$$\mathbf{E}(\mathbf{r},t) = \mathbf{E}^{(1)}_{l}(\mathbf{r},t) + \mathbf{E}_{d1}(\mathbf{r},t) + \mathbf{E}^{(1)}_{d2}(\mathbf{r},t), \text{(in region II)}$$

$$\mathbf{E}(\mathbf{r},t) = \mathbf{E}^{(2)}_{p}(\mathbf{r},t) + \mathbf{E}_{d1}(\mathbf{r},t) + \mathbf{E}^{(2)}_{d2}(\mathbf{r},t), \text{(in region IV)}.$$

There are a localized field and diffusion fields in the emitted field for region II. While the emitted field composes of a propagating field and diffusion fields in region IV.

From the above discussion we know that the main parts of the emission field can be written as

$$\mathbf{E}(\mathbf{r},t) = \begin{cases} \mathbf{E}^{(1)}_{l1}(\mathbf{r},t)+\mathbf{E}^{(1)}_{l2}(\mathbf{r},t)+\mathbf{E}_{d1}(\mathbf{r},t)+\mathbf{E}^{(1)}_{d2}(\mathbf{r},t) & \text{(region I)} \\ \mathbf{E}^{(1)}_{l}(\mathbf{r},t)+\mathbf{E}_{d1}(\mathbf{r},t)+\mathbf{E}^{(1)}_{d2}(\mathbf{r},t) & \text{(region II)} \\ \mathbf{E}^{(1)}_{l}(\mathbf{r},t)+\mathbf{E}^{(2)}_{p}(\mathbf{r},t)+\mathbf{E}_{d1}(\mathbf{r},t)+\mathbf{E}_{d2}(\mathbf{r},t) & \text{(region III)} \\ \mathbf{E}^{(2)}_{p}(\mathbf{r},t)+\mathbf{E}_{d1}(\mathbf{r},t)+\mathbf{E}^{(2)}_{d2}(\mathbf{r},t) & \text{(region IV)} \\ \mathbf{E}^{(2)}_{p1}(\mathbf{r},t)+\mathbf{E}^{(2)}_{p2}(\mathbf{r},t)+\mathbf{E}_{d1}(\mathbf{r},t)+\mathbf{E}^{(2)}_{d2}(\mathbf{r},t) & \text{(region V)} \end{cases} . \quad (17)$$

The emission field from the excited atom is characterized by three different fields: the localized field, the propagating field and the diffusion field. The amplitudes of these fields depend strongly on the relative position $\omega_{2c}$. In Figure 6 we plot the amplitudes of the localized field and the propagating field as functions of the relative position of the middle level $|2\rangle$ from the band edge for fixed distance from the atom $r = \sqrt{A/\beta}$ and at the fixed time $t = 3/\beta$.

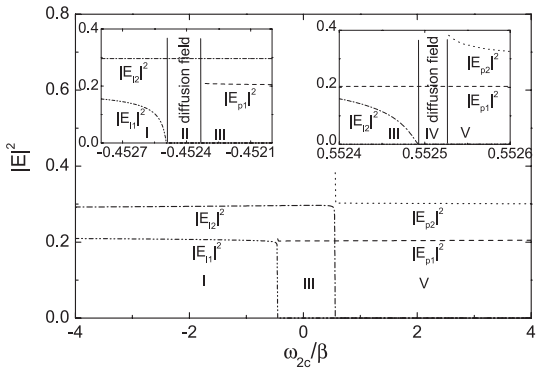


**Fig. 6.** The amplitude square (in arbitrary unit) of the localized field and propagating field as function of the relative position $\omega_{2c}$ with $\omega_c = 100\beta$, $\Omega = 0.5\beta$, $\omega_{L12} = 0$, $r\sqrt{\beta/A} = 1$, and $\beta t = 3$.

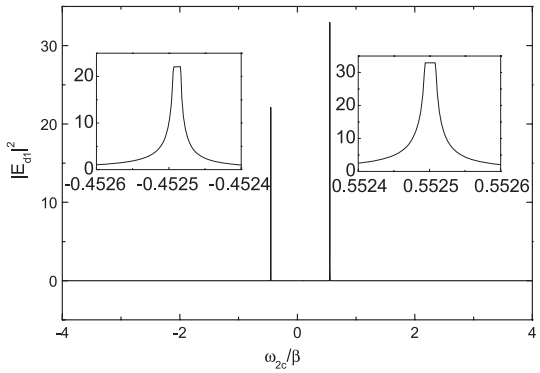


**Fig. 7.** The amplitude square (in arbitrary unit) of the diffusion field $\mathbf{E}_{d1}(\mathbf{r},t)$ as function of the relative position $\omega_{2c}$ with $\omega_c = 100\beta$, $\Omega = 0.5\beta$, $\omega_{L12} = 0$, $r\sqrt{\beta/A} = 1$, and $\beta t = 3$.

From Figure 6, we found the amplitudes of the localized fields $\mathbf{E}_l^{(1)}(\mathbf{r},t)$ decrease as $\omega_{2c}$ increases and the localized field $\mathbf{E}_{l1}^{(1)}(\mathbf{r},t)$ (or $\mathbf{E}_{l2}^{(1)}(\mathbf{r},t)$) will decreases to zero and vanishes when $\omega_{2c}$ changes from region I to region II (or from region III to region IV). While, when the relative position $\omega_{2c}$ changes from region II to region III (or from region IV to region V), there is a pronounced switch-on effect for the propagating field $\mathbf{E}_{p1}^{(2)}(\mathbf{r},t)$ (or $\mathbf{E}_{p2}^{(2)}(\mathbf{r},t)$). These sudden increases of the propagating field can be used to design an active optical multi-channel micro-sized switch.

Although both the fields $\mathbf{E}_{d1}(\mathbf{r},t)$ and $\mathbf{E}_{d2}(\mathbf{r},t)$ are the diffusion fields, their contributions to the emitted field in different region of the middle level $|2\rangle$ are different. We plot the amplitudes of the diffusion field $\mathbf{E}_{d1}(\mathbf{r},t)$ in Figure 7 and the diffusion field $\mathbf{E}_{d2}(\mathbf{r},t)$ in Figure 8, respectively, as functions of the relative position of the middle level $|2\rangle$ from the band edge for fixed distance from the atom $r = \sqrt{A/\beta}$ and at the fixed time $t = t_0 = 3/\beta$. From Figure 7, we note that the amplitudes of the diffusion field $\mathbf{E}_{d1}(\mathbf{r},t)$ in regions II and IV are almost constant and extremely strong (several hundred times stronger than that in other regions). The diffusion field $\mathbf{E}_{d1}(\mathbf{r},t)$ in regions I, III and V are extremely small and can be neglected. The amplitude of the diffusion field $\mathbf{E}_{d2}(\mathbf{r},t)$ is zero for the middle level $|2\rangle$ being in regions II and IV, while it is not zero and much larger than the amplitude of $\mathbf{E}_{d1}(\mathbf{r},t)$ for the middle level $|2\rangle$ being in regions I, III and V (see Fig. 8). When the middle level $|2\rangle$ is far away from the regions II and IV, the amplitude of $\mathbf{E}_{d2}(\mathbf{r},t)$ is small (but much larger than $\mathbf{E}_{d1}(\mathbf{r},t)$) because the diffusion field $\mathbf{E}_{d2}(\mathbf{r},t)$ has already decayed at time $t_0$.

Considering the process of the middle level $|2\rangle$ moves from deep in the band gap to deep in the transmitting band, we can get the following picture of the energy translation among the three different fields. When the relative position $\omega_{2c}$ increases from region I to region II, the amplitude of the localized field $\mathbf{E}_{l1}^{(1)}(\mathbf{r},t)$ tends to zero and disappears, and the diffusion field appears. The corresponding energy of the localized field has been transferred to the

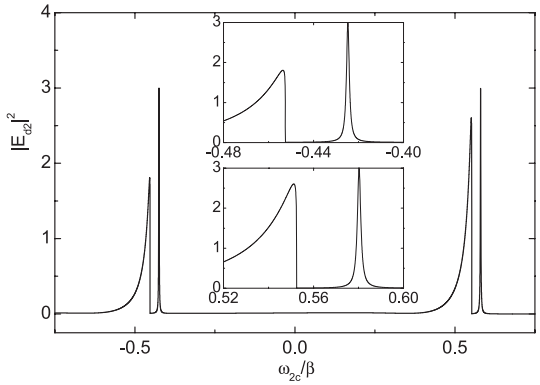


**Fig. 8.** The amplitude square (in arbitrary unit) of the diffusion field $\mathbf{E}_{d2}(\mathbf{r},t)$ as function of the relative position $\omega_{2c}$ with $\omega_c = 100\beta$, $\Omega = 0.5\beta$, $\omega_{L12} = 0$, $r\sqrt{\beta/A} = 1$, and $\beta t = 3$.

diffusion field $\mathbf{E}_{d1}(\mathbf{r},t)$ (see Figs. 6 and 7). As $\omega_{2c}$ changes from region II to region III, the propagating field $\mathbf{E}_{p1}^{(2)}(\mathbf{r},t)$ begins to appear and the corresponding energy of the diffusion field $\mathbf{E}_{d1}(\mathbf{r},t)$ is transferred to $\mathbf{E}_{p1}^{(2)}(\mathbf{r},t)$. Similarly, as $\omega_{2c}$ increases from region III through region IV to region V, the same process goes on among the localized field $\mathbf{E}_{l2}^{(1)}(\mathbf{r},t)$, the diffusion field $\mathbf{E}_{d1}(\mathbf{r},t)$ and the propagating field $\mathbf{E}_{p2}^{(2)}(\mathbf{r},t)$ (see Figs. 6 and 7). The disappearance of the localized field in the present case is caused by the anisotropic dispersion relation and this property does not exist for an isotropic dispersion relation. For isotropic case, the one-dimensional dispersion relation results in a singularity in the density of state (DOS), and any weak potential will lead to localization for electron [30]. John and Wang mentioned the analogous localization for photon in photonic crystal, and got the concept of the 'bound photon-atom state' [5]. Kofman et al. examined the same question for a more general case [8]. So the localized field always exists in the isotropic case.

The properties of the emission field also depend on the external driving field. From the above discussion in the previous section, we know that for fixed relative position $\omega_{2c}$, the corresponding dressed states can change from region I through region II to region III (or from region V

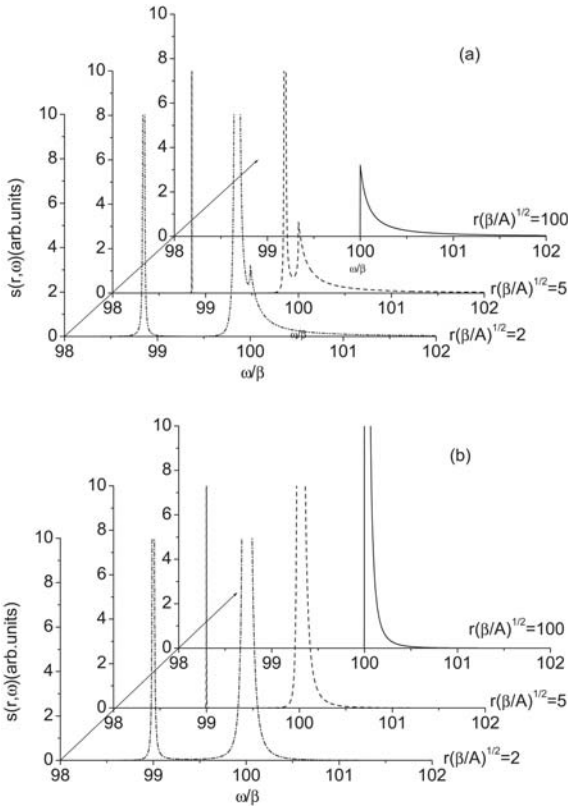


**Fig. 9.** The spectra of spontaneous emission from the excited atom for $\omega_c = 100\beta$, $\Omega = 0.5\beta$, $\omega_{L12} = 0$, and (a) $\omega_{2c} = -0.6\beta$ (region I), (b) $\omega_{2c} = -0.452485\beta$ (region II) with different distance from atom.

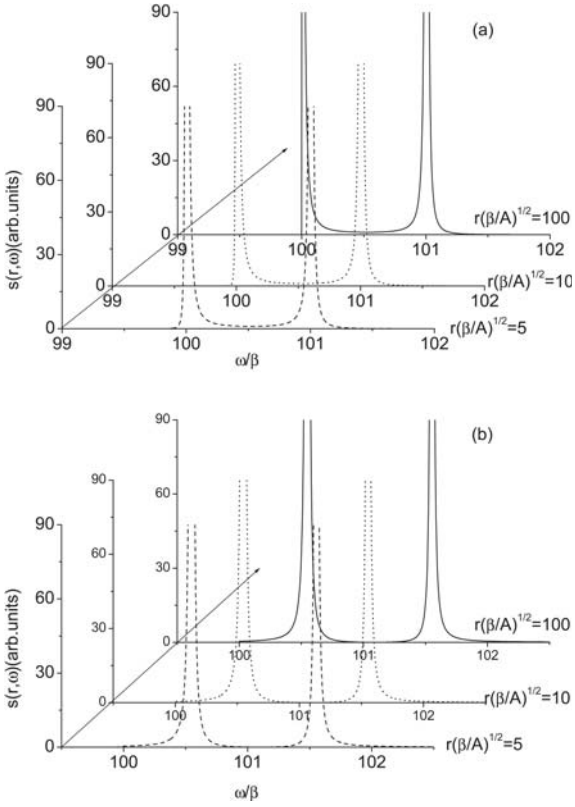


**Fig. 10.** The spectra of spontaneous emission from the excited atom for $\omega_c = 100\beta$, $\Omega = 0.5\beta$, $\omega_{L12} = 0$, and (a) $\omega_{2c} = 0.5525\beta$ (region IV), (b) $\omega_{2c} = 1.1\beta$ (region V) with different distance from atom.

through region IV to region III) as the intensity $\Omega$ of the driving field increases. Furthermore, we found that the main components of the emission field are so different in the five regions from equations (17). So we can change or so much as control the properties of the emission field with the help of choosing suitable intensity of the external driving field.

## 5 Spontaneous emission spectrum

Photonic crystals can affect strongly the spontaneous spectrum of the excited atom. From Appendix D the radiation spectrum $S(\mathbf{r}, \omega)$ can be written as

$$\mathbf{S}(\mathbf{r}, \boldsymbol{\omega}) = \begin{cases} |\mathbf{F}_1(\mathbf{r}, \boldsymbol{\omega}) + \mathbf{F}_3(\mathbf{r}, \boldsymbol{\omega})|^2 & \text{(region I)} \\ |\mathbf{F}_1(\mathbf{r}, \boldsymbol{\omega}) + \mathbf{F}_3(\mathbf{r}, \boldsymbol{\omega})|^2 & \text{(region II)} \\ |\mathbf{F}_1(\mathbf{r}, \boldsymbol{\omega}) + \mathbf{F}_2(\mathbf{r}, \boldsymbol{\omega}) + \mathbf{F}_3(\mathbf{r}, \boldsymbol{\omega})|^2 & \text{(region III)} \\ |\mathbf{F}_2(\mathbf{r}, \boldsymbol{\omega}) + \mathbf{F}_3(\mathbf{r}, \boldsymbol{\omega})|^2 & \text{(region IV)} \\ |\mathbf{F}_2(\mathbf{r}, \boldsymbol{\omega}) + \mathbf{F}_3(\mathbf{r}, \boldsymbol{\omega})|^2 & \text{(region V)} \end{cases} . \quad (18)$$

Where the functions $\mathbf{F}_1(\mathbf{r}, \boldsymbol{\omega})$, $\mathbf{F}_2(\mathbf{r}, \boldsymbol{\omega})$ and $\mathbf{F}_3(\mathbf{r}, \boldsymbol{\omega})$ are given in Appendix D (see Eqs. (D.3), (D.4) and (D.5)). If the middle level $|2\rangle$ is within regions I, II or III, $\mathbf{F}_3(\mathbf{r}, \boldsymbol{\omega})$ will be negligible small compared to $\mathbf{F}_{1,2}(\mathbf{r}, \boldsymbol{\omega})$.

In Figures 9 and 10, we plot the emission spectra $s(r, \omega) = \mathbf{S}(\mathbf{r}, \boldsymbol{\omega})|A|^2/|\mathbf{E}_0(\mathbf{r})|^2$ of spontaneous emission from the excited atom for $\omega_c = 100\beta$, $\omega_{L12} = 0$,and $\Omega = 0.5\beta$ with different relative positions between the middle level $|2\rangle$ and the band edge $\omega_{2c}$ and different distance from the atom $r$. When the relative position of the middle level $|2\rangle$ from the band edge $\omega_{2c}$ changes, the emission spectrum changes.

When the middle level $|2\rangle$ is within region I, there are the localized field and the diffusion field in the emitted field. The emission spectra $s(r, \omega)$ with different distance $r$ are plotted in Figure 9a. The emission spectrum is composed of two singularities due to two characteristic localized modes and one small peak at the band edge corresponding to the diffusion field for small $r$. The part of the emitted field with the frequency being in the band gap is localized, the corresponding energy is limited near the atom. As the distance $r$ increases, the amplitude corresponding to the part of $s(r, \omega)$ with frequency being in the band gap drops exponentially and becomes narrow with increasing distance from the atom $r$. So the part of the emission spectrum with frequencies being in the band gap is composed of two lines instead of two singularities corresponding to two characteristic localized modes for large $r$, and the two lines will disappear if $r$ large enough. On

the other hand, due to all energy of the emitted field with frequency being in the traveling band can propagate out, the corresponding part of the emission spectrum does not change with the distance from the atom. So we found the small peak corresponding to the diffusion field is at the band edge and does not change with the distance from the atom. In results, the total emission spectrum is dependent on the distance from the atom (the location of the observer).

As for the middle level $|2\rangle$ is within region II, there are the localized field and the diffusion field in the emitted field. The emission spectrum is composed of one singularity within the band gap due to one characteristic localized mode and one large peak at the band edge corresponding to the diffusion field. As the distance $r$ increases, the amplitude of the singularity within the band gap drops exponentially and becomes narrow to one line which will vanish if $r$ large enough. While the large peak at the band edge does not change for different distance from the atom $r$ (see Fig. 9b). Comparing Figure 9a with Figure 9b, the spectrum corresponding to the diffusion field in region II is extremely large than that in region I due to the amplitudes of the diffusion field $\mathbf{E}_{d1}(\mathbf{r}, t)$ in regions II and IV are almost constant and extremely strong (several hundred times stronger than that in other regions).

When the middle level $|2\rangle$ is within region III, there are the localized field, the propagating field and the diffusion field in the emitted field. In this region, the peak of the diffusion field at frequency $\omega_c$ is very small and it is covered by the large peak for the propagating field. So the emission spectrum is mainly composed of one singularity within the band gap due to one characteristic localized mode and one large peak with frequency being in the traveling band corresponding to the propagating field. The peak for the propagating field does not change for different distance from the atom $r$ because the energy of the propagating field with frequency being in the traveling band can propagate out.

When the middle level $|2\rangle$ is within region IV, there are the propagating field with frequency being in the traveling band and the diffusion field in the emitted field. Similar to region II, the amplitude of the diffusion field $\mathbf{E}_{d1}(\mathbf{r}, t)$ in region IV is also extremely strong (several hundred times stronger than that in other regions I, III, V). So in the emission spectrum there are obviously one peak at the band edge corresponding to the diffusion field and one peak with frequency being in the traveling band corresponding to the propagating field (see Fig. 10a). The total emission spectrum does not change for different distance from the atom $r$ because both the energy of the diffusion field and the propagating field can propagate out.

When the middle level $|2\rangle$ is within region V, there are the propagating field with frequency being in the traveling band and the diffusion field in the emitted field. Similar to region III, the amplitude of the diffusion field in region V is so small that the peak of the diffusion field at frequency $\omega_c$ is covered by the large peak for the propagating field. So in the emission spectrum there are obviously two large peaks with frequencies being in the traveling band corresponding to two propagating field modes (see Fig. 10b). The total emission spectrum does not change for different distance from the atom $r$ because both the energy of the diffusion field and the propagating field can propagate out.

It is well-known that in free space, when a two-level excited atom decays by spontaneous emission to its ground state, the spectrum of the emitted radiation has a Lorentzian shape as a function of frequency. The emission spectrum for a ladder three-level atomic system with external driving field was studied by Zhu in reference [26], and the dark line, non-Lorentzian shape are found in the emission spectrum due to quantum interference. The common characteristic of these spectra is that the spectra are independent on the position of the observer in space. For present case, the emission spectra are more complex due to the influence of photonic crystal and the external driving field. It is obviously that the emission spectra in some regions are strongly related with the distance of a particular space point $\mathbf{r}$ from the atom.

## 6 Conclusions

We have studied the properties of the spontaneous radiation from a ladder three-level atom embedded in a three-dimensional anisotropic photonic crystal with an external driving field. As a special environment, photonic crystals play an important role in the spontaneous emission of the excited atom. It is found that the properties of the spontaneous emission and the emitted field are dependent strongly on the relative position of the middle level from the band edge (five regions). We have also analyzed the influence of the external driving field on the spontaneous emission, the emitted field and the emission spectrum. Due to the Autler-Townes splitting by the action of the driving field, the external driving field can affect the properties of the spontaneous emission and the emitted field. The population exchanged between the upper and the middle levels decreases as the detuning of the external driving field frequency from the corresponding transition frequency increases. The properties of the emission field can be changed or so much as controlled by choosing suitable intensity of the external driving field. The emission spectra in different regions are different due to the different components of the emission field in corresponding regions. The emission spectrum is more complex, and dependent on the location of the observer in this case.

This work was supported in part by the National Natural Science Foundation of China (Grant No. 10674103, 60507008), the Shanghai Phosphor Tracing Plan (Grant No. 04QMH1407) and the Quantum Control Project of Shanghai Science Committee.

## Appendix A: The calculation of Γ

For the model near the band edge, the coupling constant $g_k$ can be approximated by

$$g_k = \frac{\omega_2 d_2}{\hbar}\sqrt{\frac{\hbar}{2\varepsilon_0\omega_k V_0}}\mathbf{e}_k \cdot \mathbf{u}_d. \tag{A.1}$$

We can calculate $\Gamma$ in equation (6) as follows

$$\begin{aligned}\Gamma &= \sum_{k,\mathbf{e}_k} \frac{g_k^2}{s+i(\omega_k-\omega_2)} \\ &= \frac{(\omega_2 d_2)^2}{2\epsilon_0\hbar V_0}\sum_{k,\mathbf{e}_k}\frac{(\mathbf{e}_k\cdot\mathbf{u}_d)(\mathbf{e}_k\cdot\mathbf{u}_d)}{\omega_k[s+i(\omega_k-\omega_2)]} \\ &= \frac{(\omega_2 d_2)^2}{2\epsilon_0\hbar V_0}\sum_{k}\frac{1-(\mathbf{k}\cdot\mathbf{u}_d)^2/k^2}{\omega_k[s+i(\omega_k-\omega_2)]} \\ &= \frac{(\omega_2 d_2)^2}{16\pi^3\epsilon_0\hbar}\iiint\frac{[1-(\mathbf{k}\cdot\mathbf{u}_d)^2/k^2]d^3\mathbf{k}}{\omega_k[s+i(\omega_k-\omega_2)]} \end{aligned} \tag{A.2}$$

where we have replaced the sum by an integral via $\sum_k \longrightarrow \frac{V_0}{(2\pi)^3}\iiint d^3\mathbf{k}$, and $\sum_{\mathbf{e}_k}(\mathbf{e}_k\cdot\mathbf{u}_d)(\mathbf{e}_k\cdot\mathbf{u}_d) = 1-(\mathbf{k}\cdot\mathbf{u}_d)\cdot(\mathbf{k}\cdot\mathbf{u}_d)/k^2$. Near the band edge, the dispersion relation may be expressed approximately by $\omega_k = \omega_c + A|\mathbf{k}-\mathbf{k}_0^j|^2$. The integration over $\mathbf{k}$ has to be carried out around the direction of each $\mathbf{k}_0^j$ because of the anisotropy of a three-dimensional photonic crystal. The angle between the dipole vector of the atom and the $j$th $\mathbf{k}_0^j$ is $\theta_j$. The angle between the dipole and $\mathbf{k}$ near $\mathbf{k}_0^j$ is replaced approximately by $\theta_j$. We calculate $\Gamma$ as follows

$$\begin{aligned}\Gamma &= \frac{(\omega_2 d_2)^2}{16\pi^3\epsilon_0\hbar}\iiint\frac{d^3\mathbf{k}}{\omega_k[s+i(\omega_k-\omega_2)]}\left[1-\frac{(\mathbf{k}\cdot\mathbf{u}_d)^2}{k^2}\right] \\ &= \frac{(\omega_2 d_2)^2}{16\pi^3\epsilon_0\hbar}\left(\sum_j\sin^2\theta_j\right) \\ &\quad\times\iiint_j\frac{d^3\mathbf{q}}{(\omega_c+A|\mathbf{q}|^2)[s+i(\omega_c-\omega_2+A|\mathbf{q}|^2)]} \\ &= \frac{(\omega_2 d_2)^2}{4\pi^2\epsilon_0\hbar}\left(\sum_j\sin^2\theta_j\right) \\ &\quad\times\int_0^\infty\frac{q^2dq}{(\omega_c+Aq^2)[s+i(\omega_c-\omega_2+Aq^2)]} \\ &= -\frac{(\omega_2 d_2)^2}{8\pi^2\epsilon_0\hbar A^{3/2}}\left(\sum_j\sin^2\theta_j\right) \\ &\quad\times\frac{i}{\sqrt{\omega_c}+\sqrt{-is-(\omega_2-\omega_c)}}. \end{aligned} \tag{A.3}$$

Consequently, we have

$$\Gamma = -\frac{i\beta^{3/2}}{\sqrt{\omega_c}+\sqrt{-is-(\omega_2-\omega_c)}} \tag{A.4}$$

with $\beta^{3/2} = (\omega_2 d_2)^2\sum_j\sin^2\theta_j/(8\pi\epsilon_0\hbar A^{3/2})$. The local density of modes (A.4) is a result of an approximation. A rather general model has been proposed by Kofman et al. [8], in which a cut-off-smoothing parameter is used to indicate different cases. For example, the case of large cut-off-smoothing parameter corresponds to the anisotropic model.

## Appendix B: The calculation of the amplitudes A(t) and B(t)

For convenience in the following calculation, we define functions $f_1(x)$, $f_2(x)$, $f_3(x)$, $f_4(x)$, $f_5(x)$, $f_6(x)$, $G(x)$ and $H(x)$ as follows

$$G(x) = \left(x-\frac{i}{\sqrt{\Omega_c}+\sqrt{-ix-\Omega_{2c}}}\right)(x-i\Omega_{L12})+W^2 \tag{B.1}$$

$$H(x) = \left(x-\frac{i}{\sqrt{\Omega_c}-i\sqrt{ix+\Omega_{2c}}}\right)(x-i\Omega_{L12})+W^2 \tag{B.2}$$

$$f_1(x) = WA_1(0)+(x-i\Omega_{L12})A_2(0) \tag{B.3}$$

$$f_2(x) = A_1(0)\left(x-\frac{i}{\sqrt{\Omega_c}+\sqrt{-ix-\Omega_{2c}}}\right)-WA_2(0) \tag{B.4}$$

$$f_3(x) = A_1(0)\left(x-\frac{i}{\sqrt{\Omega_c}-i\sqrt{ix+\Omega_{2c}}}\right)-WA_2(0) \tag{B.5}$$

$$\begin{aligned}f_4(x) = \Bigg\{&\left[(x-i\Omega_{2c})(\Omega_c-ix)+i\sqrt{\Omega_c}\right](x-i\Omega_{2c}+i\Omega_{L12}) \\ &+W^2\Omega_c-ix\Bigg\}^2+ix(x-i\Omega_{2c}+i\Omega_{L12})^2\end{aligned} \tag{B.6}$$

$$\begin{aligned}f_5(x) = {}&i^{1/2}\sqrt{x}(\Omega_c-ix)(-x+i\Omega_{2c}-i\Omega_{L12}) \\ &\times[WA_1(0)+(-x+i\Omega_{2c}-i\Omega_{L12})A_2(0)]\end{aligned} \tag{B.7}$$

$$\begin{aligned}f_6(x) = {}&i^{1/2}\sqrt{x}W(\Omega_c-ix) \\ &\times[-(-x+i\Omega_{2c}-i\Omega_{L12})A_2(0)-WA_1(0)]\end{aligned} \tag{B.8}$$

where $x=\frac{s}{\beta}$, $\Omega_c=\frac{\omega_c}{\beta}$, $\Omega_{2c}=\frac{\omega_{2c}}{\beta}$, $\Omega_{L12}=\frac{\omega_{L12}}{\beta}$, $W=\frac{\Omega}{\beta}$. Using the inverse Laplace transform, the amplitude $A(t)$ can be written as

$$\begin{aligned}A_1(t) &= \frac{e^{-i\omega_{L12}t}}{2\pi i}\int_{\sigma-i\infty}^{\sigma+i\infty}A_1(s-i\omega_{L12})e^{st}ds \\ &= \frac{e^{-i\omega_{L12}t}}{2\pi i}\int_{\sigma'-i\infty}^{\sigma'+i\infty} \\ &\quad\times\frac{A_1(0)\left(x-\frac{i}{\sqrt{\Omega_c}+\sqrt{-ix-\Omega_{2c}}}\right)-WA_2(0)}{\left(x-\frac{i}{\sqrt{\Omega_c}+\sqrt{-ix-\Omega_{2c}}}\right)(x-i\Omega_{L12})+W^2}e^{x\beta t}dx \\ &= \sum_j\frac{f_2(x_j^{(1)})}{G'(x_j^{(1)})}e^{x_j^{(1)}\beta t-i\omega_{L12}t} \\ &\quad-\frac{e^{-i\omega_{L12}t}}{2\pi i}\left[\int_{i\Omega_{2c}-\infty}^{i\Omega_{2c}+0}+\int_{i\Omega_{2c}+0}^{-i\infty+0}\right] \\ &\quad\times\frac{A_1(0)\left(x-\frac{i}{\sqrt{\Omega_c}+\sqrt{-ix-\Omega_{2c}}}\right)-WA_2(0)}{\left(x-\frac{i}{\sqrt{\Omega_c}+\sqrt{-ix-\Omega_{2c}}}\right)(x-i\Omega_{L12})+W^2}e^{x\beta t}dx\end{aligned} \tag{B.9}$$

$$\frac{e^{-i\omega_{L12}t}}{2\pi i}\int_{i\Omega_{2c}+0}^{-i\infty+0}\frac{A_1(0)\left(x-\frac{i}{\sqrt{\Omega_c}+\sqrt{-ix-\Omega_{2c}}}\right)-WA_2(0)}{\left(x-\frac{i}{\sqrt{\Omega_c}+\sqrt{-ix-\Omega_{2c}}}\right)(x-i\Omega_{L12})+W^2}e^{x\beta t}dx$$
$$=\frac{e^{-i\omega_{L12}t}}{2\pi i}\int_{i\Omega_{2c}}^{-i\infty}\frac{A_1(0)\left(x-\frac{i}{\sqrt{\Omega_c}-i\sqrt{ix+\Omega_{2c}}}\right)-WA_2(0)}{\left(x-\frac{i}{\sqrt{\Omega_c}-i\sqrt{ix+\Omega_{2c}}}\right)(x-i\Omega_{L12})+W^2}e^{x\beta t}dx$$
$$=-\frac{e^{-i\omega_{L12}t}}{2\pi i}\int_{i\Omega_{2c}-\infty}^{i\Omega_{2c}}\frac{A_1(0)\left(x-\frac{i}{\sqrt{\Omega_c}-i\sqrt{ix+\Omega_{2c}}}\right)-WA_2(0)}{\left(x-\frac{i}{\sqrt{\Omega_c}-i\sqrt{ix+\Omega_{2c}}}\right)(x-i\Omega_{L12})+W^2}e^{x\beta t}dx-\sum_j\frac{f_3(x_j^{(2)})}{H'(x_j^{(2)})}e^{x_j^{(2)}\beta t-i\omega_{L12}t} \quad \text{(B.10)}$$

$$A_1(t)=e^{-i\omega_{L12}t}\left[\sum_j\frac{f_2(x_j^{(1)})}{G'(x_j^{(1)})}e^{x_j^{(1)}\beta t}+\sum_j\frac{f_3(x_j^{(2)})}{H'(x_j^{(2)})}e^{x_j^{(2)}\beta t}\right]+\frac{e^{-i\omega_{L12}t}}{2\pi i}\int_{i\Omega_{2c}-\infty}^{i\Omega_{2c}}e^{x\beta t}dx$$
$$\times\left[\frac{A_1(0)\left(x-\frac{i}{\sqrt{\Omega_c}-i\sqrt{ix+\Omega_{2c}}}\right)-WA_2(0)}{\left(x-\frac{i}{\sqrt{\Omega_c}-i\sqrt{ix+\Omega_{2c}}}\right)(x-i\Omega_{L12})+W^2}-\frac{A_1(0)\left(x-\frac{i}{\sqrt{\Omega_c}+\sqrt{-ix-\Omega_{2c}}}\right)-WA_2(0)}{\left(x-\frac{i}{\sqrt{\Omega_c}+\sqrt{-ix-\Omega_{2c}}}\right)(x-i\Omega_{L12})+W^2}\right]$$
$$=e^{-i\omega_{L12}t}\left[\sum_j\frac{f_2(x_j^{(1)})}{G'(x_j^{(1)})}e^{x_j^{(1)}\beta t}+\sum_j\frac{f_3(x_j^{(2)})}{H'(x_j^{(2)})}e^{x_j^{(2)}\beta t}+\frac{e^{i\omega_{2c}t}}{\pi}\int_0^\infty\frac{f_6(x)}{f_4(x)}e^{-x\beta t}dx\right] \quad \text{(B.11)}$$

where $x_j^{(1)}$ are the roots of equation $G(x)=0$ in the region $(\mathrm{Re}(x)>0)$ or $(\mathrm{Im}(x)>\Omega_{2c})$. The real number $\sigma'$ is chosen so that $x=\sigma'$ lies to the right of all the singularity $x_j^{(1)}$

*see equations (B.10) above*

where $x_j^{(2)}$ is the roots of equation $H(x)=0$ in the region: $(\mathrm{Re}(x)<0$ and $\mathrm{Im}(x)<\Omega_{2c})$

*see equations (B.11) above.*

Similarly, using the inverse Laplace transform, the amplitude $A_2(t)$ can be written as

$$A_2(t)=\frac{1}{2\pi i}\int_{\sigma-i\infty}^{\sigma+i\infty}A_2(s)e^{st}ds$$
$$=\sum_j\frac{f_1(x_j^{(1)})}{G'(x_j^{(1)})}e^{x_j^{(1)}\beta t}+\sum_j\frac{f_1(x_j^{(2)})}{H'(x_j^{(2)})}e^{x_j^{(2)}\beta t}$$
$$+\frac{e^{i\omega_{2c}t}}{\pi}\int_0^\infty\frac{f_5(x)}{f_4(x)}e^{-x\beta t}dx. \quad \text{(B.12)}$$

## Appendix C: The calculation of the radiation field E(r, t)

For the model near the band edge, the amplitude of the radiated field at a particular space point $\mathbf{r}$ can be approximated by [29]

$$\mathbf{E}(\mathbf{r},t)=\sum_k\sqrt{\frac{\hbar\omega_k}{2\varepsilon_0V_0}}e^{-i(\omega t-\mathbf{k}\cdot\mathbf{r})}B_k(t)\mathbf{e}_k$$
$$=\sum_k\frac{\omega_2d_2}{2\varepsilon_0V_0}e^{-i(\omega t-\mathbf{k}\cdot\mathbf{r})}\left[\int_0^tA_2(t')e^{i(\omega_k-\omega_{23})t'}dt'\right]$$
$$\times\left[\mathbf{u}_d-\frac{\mathbf{k}(\mathbf{k}\cdot\mathbf{u}_d)}{k^2}\right]$$
$$=\frac{\omega_2d_2}{16\pi^3\varepsilon_0}\sum_je^{i\mathbf{k}_0^j\cdot\mathbf{r}}\left[\mathbf{u}_d-\frac{\mathbf{k}_0^j(\mathbf{k}_0^j\cdot\mathbf{u}_d)}{(k_0^j)^2}\right]$$
$$\times\iiint d^3\mathbf{q}e^{-i(\omega_qt-\mathbf{q}\cdot\mathbf{r})}\left[\int_0^tA_2(t')e^{i(\omega_q-\omega_2)t'}dt'\right] \quad \text{(C.1)}$$

where we have used $\mathbf{q}=\mathbf{k}-\mathbf{k}_0^j$, $d^3\mathbf{q}=d^3\mathbf{k}$, and have replaced the sum by an integral via $\sum_{\mathbf{k}}\to\frac{V}{(2\pi)^3}\iiint d^3\mathbf{k}$.

Suppose $A_2(t')=e^{x\beta t'}$, we have

$$\iiint d^3\mathbf{q}e^{-i(\omega_qt-\mathbf{q}\cdot\mathbf{r})}\int_0^tA_2(t')^{i(\omega_q-\omega_{23})t'}dt'=$$
$$\frac{2\pi}{ir}\int_{-\infty}^\infty\frac{e^{(x\beta-i\omega_2)t}-e^{-i\omega_qt}}{i(\omega_q-\omega_2)+x\beta}e^{iqr}qdq \quad \text{(C.2)}$$

$$\int_{-\infty}^\infty\frac{e^{(x\beta-i\omega_2)t}}{i(\omega_q-\omega_2)+x\beta}e^{iqr}qdq=$$
$$\frac{\pi}{A}e^{(x\beta-i\omega_2)t-r\sqrt{[(\omega_c-\omega_2)-ix\beta]/A}} \quad \text{(C.3)}$$

$$\frac{\omega_2 d_2}{16\pi^3\varepsilon_0}\sum_j e^{i\mathbf{k}_0^n\cdot\mathbf{r}}\left[\mathbf{u}_d-\frac{\mathbf{k}_0^j(\mathbf{k}_0^j\cdot\mathbf{u}_d)}{(k_0^j)^2}\right]\iiint d^3\mathbf{q}e^{-i(\omega_q t-\mathbf{q}\cdot\mathbf{r})}\left[\int_0^t A_2(t')e^{i(\omega_q-\omega_2)t'}dt'\right]$$

$$=\frac{\omega_2 d_2}{8\pi^2\varepsilon_0 ri}\sum_j e^{i\mathbf{k}_0^j\cdot\mathbf{r}}\left[\mathbf{u}_d-\frac{\mathbf{k}_0^j(\mathbf{k}_0^j\cdot\mathbf{u}_d)}{(k_0^j)^2}\right]\int_{-\infty}^{\infty}\frac{e^{(x\beta-i\omega_2)t}-e^{-i\omega_q t}}{i(\omega_q-\omega_2)+x\beta}e^{iqr}qdq$$

$$=\frac{\omega_2 d_2}{8\pi^2\varepsilon_0 ri}\sum_j e^{i\mathbf{k}_0^j\cdot\mathbf{r}}\left[\mathbf{u}_d-\frac{\mathbf{k}_0^j(\mathbf{k}_0^j\cdot\mathbf{u}_d)}{(k_0^j)^2}\right]$$

$$\times\left\{\frac{\pi}{A}e^{(x\beta-i\omega_2)t-r\sqrt{((\omega_c-\omega_2)-ix\beta)/A}}\Theta\left(2t\sqrt{A}(\mathrm{Re}-\mathrm{Im})\sqrt{\omega_c-\omega_2-ix\beta}-r\right)\Theta(\omega_c-\omega_2+\mathrm{Im}(x\beta))\right.$$

$$+\frac{\pi}{A}e^{(x\beta-i\omega_2)t+r\sqrt{((\omega_c-\omega_2)-ix\beta)/A}}\Theta\left(2t\sqrt{A}(\mathrm{Im}-\mathrm{Re})\sqrt{\omega_c-\omega_2-ix\beta}-r\right)\Theta(\omega_2-\omega_c-\mathrm{Im}(x\beta))$$

$$\left.+e^{-i(\omega_c t-\frac{r^2}{4At})+\frac{3}{4}\pi i}\int_{-\infty}^{\infty}\frac{\left(\rho e^{\frac{3}{4}\pi i}+\frac{r}{2At}\right)e^{-At\rho^2}}{x\beta+i(\omega_c-\omega_2)+iA\left(\rho e^{\frac{3}{4}\pi i}+\frac{r}{2At}\right)^2}d\rho\right\}. \tag{C.5}$$

---

$$\int_{-\infty}^{\infty}\frac{e^{-i\omega_q t}}{i(\omega_q-\omega_2)+x\beta}e^{iqr}qdq=$$

$$\int_{-\infty}^{\infty}\frac{(q+\frac{r}{2At})e^{-iAtq^2}e^{-i[\omega_c t-(r^2/4At)]}}{i(\omega_c-\omega_2)+iA(q+\frac{r}{2At})^2+x\beta}dq \tag{C.4}$$

with

$$\int_{-\infty}^{0}\frac{(q+\frac{r}{2At})e^{-iAtq^2}e^{-i[\omega_c t-(r^2/4At)]}}{i(\omega_c-\omega_2)+iA(q+\frac{r}{2At})^2+x\beta}dq=$$

$$\frac{\pi}{A}e^{(x\beta-i\omega_2)t-r\sqrt{[(\omega_c-\omega_2)-ix\beta]/A}}$$

$$\times\begin{cases}1 & (\mathrm{Im}(x\beta)<\omega_2-\omega_c)\\ \Theta[r+2t\sqrt{A}(\mathrm{Im}-\mathrm{Re})\sqrt{\omega_c-\omega_2-ix\beta}] & (\mathrm{Im}(x\beta)\geqslant\omega_2-\omega_c)\end{cases}$$

$$-e^{-i[\omega_c t-(r^2/4At)]+(3/4)\pi i}$$

$$\times\int_0^{\infty}\frac{\left(\rho e^{(3/4)\pi i}+\frac{r}{2At}\right)e^{-At\rho^2}}{x\beta+i(\omega_c-\omega_2)+iA\left(\rho e^{(3/4)\pi i}+\frac{r}{2At}\right)^2}d\rho$$

and

$$\int_0^{\infty}\frac{(q+\frac{r}{2At})e^{-iAtq^2}e^{-i[\omega_c t-(r^2/4At)]}}{i(\omega_c-\omega_2)+iA(q+\frac{r}{2At})^2+x\beta}dq=$$

$$-\frac{\pi}{A}e^{(x\beta-i\omega_2)t+r\sqrt{[(\omega_c-\omega_2)-ix\beta]/A}}$$

$$\times\begin{cases}\Theta[2t\sqrt{A}(\mathrm{Im}-\mathrm{Re})\sqrt{\omega_c-\omega_2-ix\beta}-r] & (\mathrm{Im}(x\beta)<\omega_2-\omega_c)\\ 0 & (\mathrm{Im}(x\beta)\geqslant\omega_2-\omega_c)\end{cases}$$

$$+e^{-i[\omega_c t-(r^2/4At)]-(1/4)\pi i}$$

$$\times\int_0^{\infty}\frac{\left(\rho e^{-(1/4)\pi i}+\frac{r}{2At}\right)e^{-At\rho^2}}{x\beta+i(\omega_c-\omega_2)+iA\left(\rho e^{-(1/4)\pi i}+\frac{r}{2At}\right)^2}d\rho.$$

Here $\Theta(x)$ is the step function for $x\geqslant 0$, $\Theta(x)=1$, and $x<0$, $\Theta(x)=0$. So we can obtain

*see equation (C.5) above.*

From equations (B.12), (C.1), and (C.5), we can calculate the radiation field $\mathbf{E}(\mathbf{r},t)$. Corresponding to each term in $A_2(t)$, we can obtain

$$\mathbf{E}(\mathbf{r},t)=\mathbf{E}^{(1)}(\mathbf{r},t)+\mathbf{E}^{(2)}(\mathbf{r},t)+\mathbf{E}^{(3)}(\mathbf{r},t). \tag{C.6}$$

(1) For the pure imaginary root $x_j^{(1)}=ib_j^{(1)}/\beta$, we have $\omega_2-b_j^{(1)}<\omega_c$. The term in $A_2(t)$ related to $x_j^{(1)}$ is $\sum_j\frac{f_1(x_j^{(1)})}{G'(x_j^{(1)})}e^{x_j^{(1)}\beta t}$. So the term $\mathbf{E}^{(1)}(\mathbf{r},t)$ in the radiation field $\mathbf{E}(\mathbf{r},t)$ can be obtained as follows:

$$\mathbf{E}^{(1)}(\mathbf{r},t)=\mathbf{E}_0(\mathbf{r})\sum_j\frac{f_1(x_j^{(1)})}{G'(x_j^{(1)})}$$

$$\times\left\{\frac{\pi}{A}e^{-i(\omega_2-b_j^{(1)})t-r\sqrt{(\omega_c-\omega_2+b_j^{(1)})/A}}\right.$$

$$\times\Theta\left(t-\frac{r}{2\sqrt{A}\sqrt{\omega_c-\omega_2+b_j^{(1)}}}\right)$$

$$\left.+e^{-i(\omega_c t-\frac{r^2}{4At})+\frac{1}{4}\pi i}\int_{-\infty}^{\infty}\frac{(\rho e^{\frac{3}{4}\pi i}+\frac{r}{2At})e^{-At\rho^2}}{(\omega_c-\omega_2+b_j^{(1)})+A(\rho e^{\frac{3}{4}\pi i}+\frac{r}{2At})^2}d\rho\right\} \tag{C.7}$$

where $\mathbf{E}_0(\mathbf{r})=\frac{\omega_2 d_2}{8\pi^2\varepsilon_0 ri}\sum_j e^{i\mathbf{k}_0^j\cdot\mathbf{r}}[\mathbf{u}_d-\frac{\mathbf{k}_0^j(\mathbf{k}_0^j\cdot\mathbf{u}_d)}{(k_0^j)^2}]$.

(2) For the complex root $x_j^{(2)} = (a_j^{(2)} + ib_j^{(2)})/\beta$, we have $\omega_2 - b_j^{(2)} > \omega_c$ and $a_j^{(2)} < 0$. The term $\sum_j \frac{f_1(x_j^{(2)})}{H'(x_j^{(2)})} e^{x_j^{(2)}\beta t}$ in $A_2(t)$ is related to $x_j^{(2)}$. So the term $\mathbf{E}^{(2)}(\mathbf{r},t)$ in the radiation field $\mathbf{E}(\mathbf{r},t)$ can be written as:

$$\mathbf{E}^{(2)}(\mathbf{r},t) = \mathbf{E}_0(\mathbf{r}) \sum_j \frac{f_1(x_j^{(2)})}{H'(x_j^{(2)})} \times \left\{ \frac{\pi}{A} e^{-i(\omega_2 + ix_j^{(2)}\beta)t - r\sqrt{(\omega_c - \omega_2 - ix_j^{(2)}\beta)/A}} \times \Theta\left( t - \frac{r}{2\sqrt{A}(\mathrm{Re} - \mathrm{Im})\sqrt{\omega_c - \omega_2 - ix_j^{(2)}\beta}} \right) + e^{-i(\omega_c t - \frac{r^2}{4At}) + \frac{1}{4}\pi i} \times \int_{-\infty}^{\infty} \frac{(\rho e^{\frac{3}{4}\pi i} + \frac{r}{2At}) e^{-At\rho^2}}{(\omega_c - \omega_2 - ix_j^{(2)}\beta) + A(\rho e^{\frac{3}{4}\pi i} + \frac{r}{2At})^2} d\rho \right\}. \quad \text{(C.8)}$$

(3) For the integration term in $A_2(t)$, we have

$$\mathbf{E}^{(3)}(\mathbf{r},t) = \frac{\mathbf{E}_0(\mathbf{r})}{\pi} \int_0^{\infty} \frac{f_5(x)}{f_4(x)} dx \left[ e^{-i(\omega_c t - \frac{r^2}{4At}) + \frac{3}{4}\pi i} \times \int_{-\infty}^{\infty} \frac{(\rho e^{\frac{3}{4}\pi i} + \frac{r}{2At}) e^{-At\rho^2}}{-x\beta + iA(\rho e^{\frac{3}{4}\pi i} + \frac{r}{2At})^2} d\rho \right]. \quad \text{(C.9)}$$

## Appendix D: The calculation of the emission spectrum $\mathbf{S}(\mathbf{r},\boldsymbol{\omega})$

The Fourier transform of the radiation field is

$$\mathbf{F}(\mathbf{r},\boldsymbol{\omega}) = \frac{1}{2\pi} \int_0^{\infty} \mathbf{E}(\mathbf{r},t) e^{i\omega t} dt. \quad \text{(D.1)}$$

So the emission spectrum $\mathbf{S}(\mathbf{r},\boldsymbol{\omega})$ can be obtained, $\mathbf{S}(\mathbf{r},\boldsymbol{\omega}) = |\mathbf{F}(\mathbf{r},\boldsymbol{\omega})|^2$. From equations (B.12) and (C.1), $\mathbf{F}(\mathbf{r},\boldsymbol{\omega})$ can be rewritten as the sum of three parts, which come from the three terms of equation (B.12):

$$\mathbf{F}(\mathbf{r},\boldsymbol{\omega}) = \mathbf{F}_1(\mathbf{r},\boldsymbol{\omega}) + \mathbf{F}_2(\mathbf{r},\boldsymbol{\omega}) + \mathbf{F}_3(\mathbf{r},\boldsymbol{\omega}). \quad \text{(D.2)}$$

(1) For the pure imaginary root $x_j^{(1)}$, we have

$$\begin{aligned} \mathbf{F}_1(\mathbf{r},\omega) &= \frac{\mathbf{E}_0(\mathbf{r})}{2\pi} \sum_j \frac{f_1(x_j^{(1)})}{G'(x_j^{(1)})} \int_{-\infty}^{\infty} \frac{q e^{iqr} dq}{i(\omega_q - \omega_2) + x_j^{(1)}\beta} \\ &\quad \times \int_0^{\infty} (e^{(x_j^{(1)}\beta - i\omega_2)t + i\omega t} - e^{-i\omega_q t + i\omega t}) dt \\ &= \frac{\mathbf{E}_0(\mathbf{r})}{2\pi} \sum_j \frac{f_1(x_j^{(1)})}{G'(x_j^{(1)})} \lim_{s\to 0^+} \int_{-\infty}^{\infty} \\ &\quad \times \frac{q e^{iqr} dq}{[-s + i(\omega - \omega_2 - ix_j^{(1)}\beta)][-s + i(\omega - \omega_q)]} \\ &= -\frac{\mathbf{E}_0(\mathbf{r})}{2A} \sum_j \frac{f_1(x_j^{(1)})}{G'(x_j^{(1)})} \\ &\quad \times \lim_{s\to 0^+} \frac{f(\omega)}{-s + i(\omega - \omega_2 - ix_j^{(1)}\beta)} \end{aligned} \quad \text{(D.3)}$$

where $\Theta(x)$ is the step function. The functions $f(\omega)$ is defined as

$$f(\omega) = e^{-r\sqrt{(\omega_c - \omega)/A}} \Theta(\omega_c - \omega) + e^{ir\sqrt{(\omega - \omega_c)/A}} \Theta(\omega - \omega_c)$$

(2) For the complex root $x_j^{(2)} = (a_j^{(2)} + ib_j^{(2)})/\beta$ , we have $\omega_2 - b_j^{(2)} > \omega_c$ and $a_j^{(2)} < 0$

$$\mathbf{F}_2(\mathbf{r},\omega) = -\frac{\mathbf{E}_0(\mathbf{r})}{2A} \sum_j \frac{f_1(x_j^{(2)})}{H'(x_j^{(2)})} \frac{f(\omega)}{i(\omega - \omega_2 - ix_j^{(2)}\beta)}. \quad \text{(D.4)}$$

(3) For the integration term in $B(t)$, we have

$$\mathbf{F}_3(\mathbf{r},\omega) = \frac{\mathbf{E}_0(\mathbf{r})}{2A\pi} \int_0^{\infty} \frac{f_5(x)}{f_4(x)} \frac{f(\omega)}{i(\omega - \omega_2 - ix\beta)} dx. \quad \text{(D.5)}$$

## References


1. E. Yablonovitch, Phys. Rev. Lett. **58**, 2059 (1987); S. John, Phys. Rev. Lett. **58**, 2486 (1987)
2. E.M. Purcell, Phys. Rev. **69**, 681 (1946); D. Kleppner, Phys. Rev. Lett. **47**, 233 (1981)
3. E. Yablonovitch, J. Opt. Soc. Am. B **10**, 283 (1993); J.D. Joannopoulos, R.D. Meade, J.N. Winn, *Photonic Crystals* (Princeton, New York, 1995)
4. S. John, T. Quang, Phys. Rev. A **50**, 1764 (1994)
5. S. John, J. Wang, Phys. Rev. Lett. **64**, 2418 (1990); S. John, J. Wang, Phys. Rev. B **43**, 12772 (1991); S. John, T. Quang, Phys. Rev. Lett. **74**, 3419 (1995); S. John, T. Quang, Phys. Rev. Lett. **76**, 1320 (1996); S. John, T. Quang, Phys. Rev. Lett. **78**, 1888 (1997); N. Vats, S. John, K. Busch, Phys. Rev. A **65**, 043808 (2002)
6. S. Bay, P. Lambropoulos, K. Molmer, Phys. Rev. Lett. **79**, 2654 (1997); P. Lambropoulos et al., Rep. Prog. Phys. **63**, 455 (2000); G.M. Nikolopoulos, P. Lambropoulos, Phys. Rev. A **61**, 053812 (2000)

7. S.-Y. Zhu, H. Chen, H. Huang, Phys. Rev. Lett. **79**, 205 (1997); S.-Y. Zhu et al., Phys. Rev. Lett. **84**, 2136 (2000); Y.P. Yang, S.-Y. Zhu, Phys. Rev. A **62**, 013805 (2000); Y.P. Yang, S.-Y. Zhu, J. Mod. Opt. **47**, 1513 (2000)
8. A.G. Kofman, G. Kurizki, B. Sherman, J. Mod. Opt. **41**, 353 (1994)
9. S. Bay, P. Lambropoulos, K. Molmer, Phys. Rev. A **55**, 1485 (1997)
10. Y.P. Yang, S.-Y. Zhu, Phys. Rev. A **61**, 043809 (2000); S.-Y. Xie, Y.P. Yang, X. Wu, Eur. Phys. J. D **13**, 129 (2001)
11. T. Quang et al., Phys. Rev. Lett. **79**, 5238 (1997)
12. Y.P. Yang et al., Phys. Lett. A **270**, 41 (2000); D.G. Angelakis, E. Paspalakis, P.L. Knight, Phys. Rev. A **64**, 013801 (2001)
13. Y.P. Yang, M. Fleischhauer, S.-Y. Zhu, Phys. Rev. E **68**, 015602R (2003); S.-Y. Zhu, G.X. Li, Y.P. Yang, F.L. Li, Europhys. Lett. **62**, 210 (2003); L. Zhou, G.X. Li, Opt. Commun. **230**, 347 (2004)
14. A.G. Kofman, G. Kurizki, Phys. Rev. A **54**, R3750 (1996); M. Lewenstein, K. Rzazewski, Phys. Rev. A **61**, 022105 (2000); Y.P. Yang, M. Fleischhauer, S.-Y. Zhu, Phys. Rev. A **68**, 022103 (2003)
15. D. Petrosyan, G. Kurizki, Phys. Rev. A **64**, 023810 (2001); I. Friedler, G. Kurizki, D. Petrosyan, Europhys. Lett. **68**, 625 (2004); I. Friedler, G. Kurizki, D. Petrosyan, Phys. Rev. A **71**, 023803 (2005)
16. X.H. Wang, Y.S. Kivshar, B.Y. Gu, Phys. Rev. Lett. **93**, 073901 (2004)
17. L. Florescu, S. John, T. Quang, R.Z. Wang, Phys. Rev. A **69**, 013816 (2004)
18. M. Florescu, S. John, Phys. Rev. A **69**, 053810 (2004); R. Wang, S. John, Phys. Rev. A **70**, 043805 (2004); D. Vujic, S. John, Phys. Rev. A **72**, 013807 (2005)
19. G.X. Li, J. Evers, C.H. Keitel, J. Phys. B **38**, 1435 (2005); P.R. Berman, Phys. Rev. Lett. **92**, 159301 (2004); A.G. Kofman, Phys. Rev. Lett. **92**, 159302 (2004)
20. A.F. Koenderink, W.L. Vos, Phys. Rev. Lett. **91**, 213902 (2003); I.S. Nikolaev, P. Lodahl, W.L. Vos, Phys. Rev. A **71**, 053813 (2005)
21. D. Englund et al., Phys. Rev. Lett. **95**, 013904 (2005)
22. S.E. Harris, Phys. Rev. Lett. **62**, 1033 (1989); S.E. Harris, J.E. Field, A. Imamoglu, Phys. Rev. Lett. **64**, 1107 (1990); K.J. Boller, A. Imamoglu, S.E. Harris, Phys. Rev. Lett. **66**, 2593 (1991); K. Hakuta, L. Micarmet, B.P. Stoicheff, Phys. Rev. Lett. **66**, 596 (1991)
23. P.L. Knight, P.M. Radmore, Phys. Lett. A **90**, 342 (1982); P. Meystre, M.S. Zubairy, Phys. Lett. A **89**, 390 (1982); G. Rempe, H. Walther, N. Klein, Phys. Rev. Lett. **58**, 353 (1987)
24. M.O. Scully, S.Y. Zhu, A. Gavridiles, Phys. Rev. Lett. **62**, 2813 (1989)
25. E.A. Harris, J.J. Macklin, Phys. Rev. A **40**, 4135 (1989); E.S. Fry et al., Phys. Rev. Lett. **70**, 3235 (1993)
26. S.-Y. Zhu, L.M. Narducci, M.O. Scully, Phys. Rev. A **52**, 4791 (1995)
27. Y.P. Yang, S.-Y. Zhu, H. Chen, H. Zheng, Physica B **279**, 155 (2000); S.-Y. Xie, Y.P. Yang, H. Chen, S.-Y. Zhu, J. Mod. Opt. **50**, 83 (2003); Y.P. Yang, M. Fleischhauer, S.-Y. Zhu, Phys. Rev. A **68**, 043805 (2003)
28. Y.P. Yang, S.-Y. Zhu, Phys. Rev. A **62**, 013805 (2000)
29. M.O. Scully, M.S. Zubairy, *Quantum Optics* (Cambridge University Press, Cambridge, 1997), Chap. 6
30. J. Callaway, *Quantum Theory of the Solid State* (Academic Press, New York, 1976), Chap. 5